Hindawi Publishing Corporation
Bioinorganic Chemistry and Applications
Volume 2006, Article ID 32896, Pages 1–10
DOI 10.1155/BCA/2006/32896

New Dihydro OO'Bis(Salicylidene) 2,2' Aminobenzothiazolyl Borate Complexes: Kinetic and Voltammetric Studies of Dimethyltin Copper Complex with Guanine, Adenine, and Calf Thymus DNA

Farukh Arjmand, Bhawana Mohani, and Shamima Parveen

Department of Chemistry, Faculty of Science, Aligarh Muslim University, Aligarh 202 002, India

Received 17 January 2005; Revised 21 March 2005; Accepted 29 March 2005

The newly synthesized ligand, dihydro OO′bis(salicylidene) 2, 2′ aminobenzothiazolyl borate (2), was derived from the reaction of Schiff base of 2-aminobenzothiazole and salicylaldehyde with KBH_4. Cu^{II} (3) and Zn^{II} (4) complexes of (2) were synthesized and further metallated with dimethyltindichloride to yield heterobimetallic complexes (5) and (6). All complexes have been thoroughly characterized by elemental analysis, and IR, NMR, EPR, and UV-Vis spectroscopy and conductance measurements. The spectroscopic data support square planar environment around the Cu^{II} atom, while the Sn^{IV} atom acquires pentacoordinate geometry. The interaction of complex (5) with guanine, adenine, and calf thymus DNA was studied by spectrophotometric, electrochemical, and kinetic methods. The absorption spectra of complex (5) exhibit a remarkable "hyperchromic effect" in the presence of guanine and calf thymus DNA. Indicative of strong binding of the complex to calf thymus DNA preferentially binds through N_7 position of guanine base, while the adenine shows binding to a lesser extent. The kinetic data were obtained from the rate constants, k_{obs}, values under pseudo-first-order conditions. Cyclic voltammetry was employed to study the interaction of complex (5) with guanine, adenine, and calf thymus DNA. The CV of complex (5) in the absence and in the presence of guanine and calf thymus DNA altered drastically, with a positive shift in formal peak potential E_{pa} and E_{pc} values and a significant increase in peak current. The positive shift in formal potentials with increase in peak current favours strong interaction of complex (5) with calf thymus DNA. The net shift in $E_{1/2}$ has been used to estimate the ratio of equilibrium constants for the binding of Cu(II) and Cu(I) complexes to calf thymus DNA.

INTRODUCTION

Present-day anticancer agents are facing challenges such as side effects, toxicity, targeting, drug delivery, acquired resistance, and cancer specificity. To overcome such problems, drugs with different molecular level action are required, and a variety of such species are under way to address these problems [1–4]. The interaction of drugs at the target site involves the DNA helix which is a sequence of bases (thymine, adenine, guanine, and cytosine). The correct conformation of the DNA helix is maintained only when adenine is paired with thymine and guanine with cytosine. A large number of articles appearing in the literature describe the interaction of metal ions with nucleic acids, giving the mechanism of action of metal-based chemotherapeutic agents that target DNA [5–10].

Developing new rational designer antitumor drugs on similar mechanisms of cisplatin, which target the cellular DNA and exhibit chemical similarity of N_7 binding site in guanine and adenine, is a most challenging area in the pharmaceutical industry. In a recent article, Lippard et al studied the theoretical binding of cisplatin to purine bases; a dominating preference for initial attack at N_7-position of guanine in comparison with adenine has been established [11]. On the basis of $\Delta G^{\ddagger}$, the activation free energy values for guanine = 24.6 kcal/mol and adenine 30.2 kcal/mol, it was predicted that guanine is 3-4 orders of magnitude more reactive towards cisplatin than adenine.

Boron compounds have received considerable attention as biologically important molecules, since boron is an essential element and is involved in nucleic acid synthesis linked to pyrimidine nucleotides [12]. They may be utilized to probe

fundamental biochemical events at the molecular level as well as in providing entirely new classes of compounds of potential medicinal value. Based upon four-coordinate boron, they generally possess sufficient hydrolytic and oxidative stability to be used in biological studies [13, 14]. The development of boron compounds for the treatment of cancer by boron neutron capture therapy (BNCT) is very significant. The closer the proximity of boron compound to tumor cell nucleus, the greater its radiobiological effect [14]. Many researchers are studying boron-containing molecules as potential delivery agents for cancer chemotherapy [15].

Boron compounds in combination with tin(IV) metal cation (hard Lewis acid), which exhibits strong affinity to the dinegative phosphate groups of DNA [16] (supportive evidence for this coordination exists both in solution [17] and in solid state [18] and tin compounds are reported to be effective against some types of cancers, such as P-338 leukemia [19, 20]), have further advantage of exhibiting therapeutic success by healing the damaged cells.

Herein, we describe the kinetics and electrochemical behavior of the representative complex (5) towards guanine, adenine, and calf thymus DNA to understand the mechanistic pathway of binding to cellular targets. These studies were carried out using UV-Vis spectroscopy and cyclic voltammetry mainly 1. The binding ability of the complex is multifold due to the presence of these metal ions which selectively bind to the target site viz copper. A transition metal ion prefers to bind to N_7 of guanine or adenine to a lesser extent of the nucleotide bases, while tin(IV) cation binds to the phosphate group of the DNA backbone [21], and boron atom provides possible cellular entrapment and retention properties in proliferating tumor cells [14].

EXPERIMENTAL

Materials and methods

All the reagents 2-aminobenzothiazol (Farak berlin, Germany), salicylaldehyde, KBH_4 (Lancaster), Calf thymus DNA, guanine, adenine (Sigma), $(CH_3)_2SnCl_2$ (Fluka), $CuCl_2 \cdot 2H_2O$, and $ZnCl_2$ (anhydrous) (Merck) were used without further purification. Microanalyses were performed by a Carlo Erba Analyzer Model 1108. Molar conductance was determined at room temperature by a Digisun electronic conductivity bridge. IR spectra (Nujol mull) (200–4000 cm^{-1}) were recorded on a Shimadzu 8201 PC spectrophotometer. ^1H and ^{13}C NMR spectra were recorded by Bruker DRX-300 spectrometer. Mass spectra were obtained on a Jeol SX-102 (FAB) spectrometer. EPR spectra were recorded on a Varian E112 spectrometer at X-band frequency (9.1 GHz) at liquid nitrogen temperature (LNT).

Cyclic voltammetry was carried out at CH instrument electrochemical analyzer. High purity H_2O and DMSO (95 : 5) was employed for the cyclic voltammetric studies with 0.4 M KNO_3 as a supporting electrolyte. A three electrode configuration was used comprising of a Pt disk working electrode, Pt wire counter electrode, and Ag/AgCl as reference electrode. Kinetic studies were carried out with a Cintra 5 UV-Vis spectrometer attached to an online data analyzer on which absorption spectra were evaluated. All experiments involving the interaction of the complex (5) with guanine, adenine, and calf thymus DNA were conducted in buffer (9.2 pH), doubly distilled water, and Tris buffer (7.5 pH), respectively. The progress of the reaction was monitored by measuring absorbance changes at 269 nm (λ_{max} of complex (5) + guanine), 260 nm (λ_{max} of adenine), and 260 nm (λ_{max} of CT-DNA), respectively. Pseudo-first-order rate constants, k_{obs}, were determined by linear least squares regression method.

Synthesis of Schiff base ligand (1)

To a solution of 2-aminobenzothiazol (5 g, 0.033 mol) in 50 mL of methanol was added (3.49 g, 0.033 mol) salicylaldehyde. The reaction mixture was refluxed for 3 hours. Yellow precipitate appears immediately on cooling, which was separated by filtration, recrystallized from methanol, and dried in vacuo over fused $CaCl_2$. Yield 7.0 g (82%) mp 120 ± 2°C (found: C, 66.16; H, 3.90; N, 10.98. $C_{14}H_{10}N_2SO$%) requires C, 66.14; H, 3.93; N, 11.02. IR/cm^{-1} (Nujol mull): 1608_{vs} (C=N), 1286 (C−OH), 753(C−S). δ_H (300 MHz, DMSO, TMS) 7.57-6.55 (ArH), 7.90-7.82 (HC=N), 10.12 (OH). δ_c 129-124 (ArC), 165 (HC=N), 152 (C−S).

Synthesis of the dihydro OO′ *bis(salicylidene)2,2′ aminobenzothiazolyl borate (2)*

To a solution of Schiff base (4.7 g, 0.018 mol) in 100 mL dry DMF was added KBH_4 (0.5 g, 0.009 mol). This reaction mixture was refluxed for circa. 10 hours in a closed assembly fitted to monitor the evolution of H_2 gas. During the course of refluxing the reaction mixture, the solution changes colour slowly from dark yellow to colorless and later turns brown. After 10 hours, the evolution of hydrogen gas ceased and light brown colored product appeared in the reaction flask. The product was filtered and washed twice with toluene and dried in vacuo over fused $CaCl_2$. Yield 3.6 g (69%) mp 260 ± 1°C (found: C, 64.88; H, 3.81; N, 10.78. $C_{28}H_{20}N_4S_2O_2B$ requires C, 64.86; H, 3.86; N, 10.81%). Mass spectrum (FAB^+): m/z 518. IR/cm^{-1} (Nujol mull): 1595_{vs} (C=N), 1391 (B−O), 2395 (B−H). $\wedge_M$ (CH_3OH): 102 Ω^{-1} cm^2 mol^{-1} (1 : 1 electrolyte). δ_H (300 MHz, DMSO, TMS) 7.55-6.52 (ArH), 7.99-7.97 (HC=N), 0.72 (B−H). δ_c 129-124 (ArC), 165 (HC=N), 114 (C−N), 153 (C−S).

Synthesis of [$C_{28}H_{22}N_4S_2O_3BCuCl$] (3)

The borate ligand (1.03 g, 0.002 mol) in 50 mL methanol was treated with $CuCl_2 \cdot 2H_2O$ (0.340 g, 0.002 mol). The reaction mixture was stirred for 2 hours and then allowed to stand overnight in refrigerator. A brown product separates out, which was isolated by filtration under vacuum. It was washed thoroughly with hexane and dried in vacuo over fused $CaCl_2$. Yield 0.57 g (54%) mp 205 ± 3°C (found: C, 53.00; H, 3.46; N, 8.84. $C_{28}H_{22}N_4S_2O_3BCuCl$ requires C, 52.99; H, 3.47; N, 8.83%). IR/cm^{-1} (Nujol mull): 1598_{vs} (C=N), 1419 (B−O), 2400 (B−H), 391 (Cu−O), 310 (Cu−Cl).

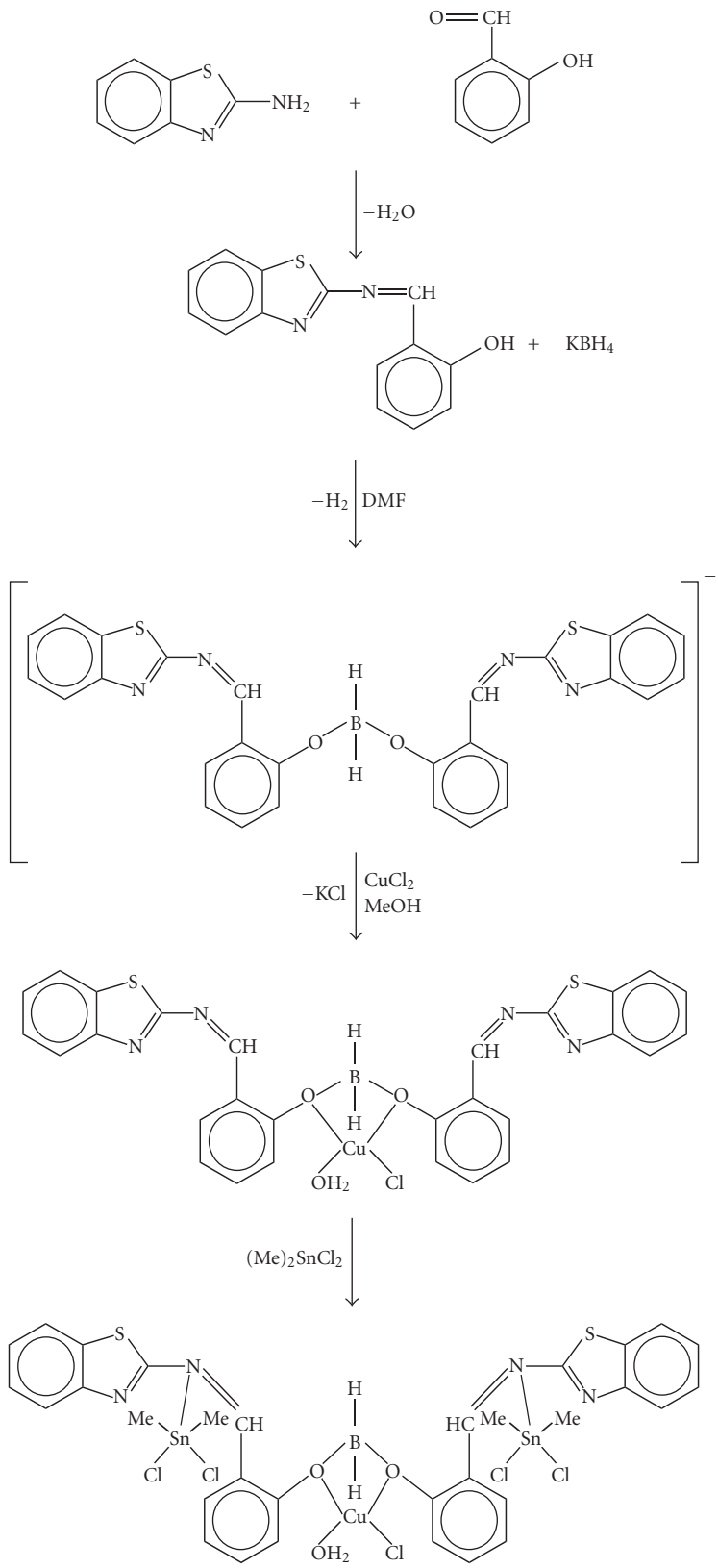
O CH
OH
S
NH2
N
+
−H2O
S
N CH
N
OH + KBH4
−H2 DMF
S
N
CH
H
B
O
O
H
CH
N
S
N
−
−KCl
CuCl2
MeOH
Cu
OH2
Cl
(Me)2SnCl2
Me
Sn
Me
Cl
Cl
HC

Scheme 1

Synthesis of **[$C_{28}H_{22}N_4S_2O_3BZnCl$]** (4)

This was synthesized by a procedure similar to that described for complex [$C_{28}H_{22}N_4S_2O_3BCuCl$] (3). Yield 0.6 g (57%) mp 220 ± 2°C (found: C, 52.84; H, 3.47; N, 8.78. $C_{29}H_{24}N_4S_2O_3BZnCl$ requires C, 52.83; H 3.45; N, 8.80%). IR/Cm^{-1} (Nujol mull): 1596_{vs} (C=N), 1423 (B−O), 2394 (B−H), 400 (Zn−O), 321 (Zn−Cl). δ_H (300 MHz, DMSO, TMS) 7.55-6.45 (ArH), 7.94–7.97 (HC=N), 0.54 (B−H). δ_c 127-125 (ArC), 165 (HC=N), 115(C−N), 151(C−S).

Synthesis of **[$C_{32}H_{34}N_4S_2O_3BCuSn_2Cl_5$]** (5)

To a solution of $C_{28}H_{22}N_4S_2O_3BCuCl$ (0.634 g, 0.001 mol) in 40 mL DMF was added $(CH_3)_2SnCl_2$ (0.438 g, 0.002 mol) in 1 : 2 molar ratio. The reaction mixture was refluxed for 48 hours on a water bath. A dark brown precipitate appears, which was isolated, filtered off, washed with hexane, and dried in vacuo over fused $CaCl_2$. Yield 0.52 g (49%) mp (dec.) 340 ± 2°C (found: C, 35.84; H, 3.16; N, 5.20. $C_{32}H_{38}N_4S_2O_7BCuSn_2Cl_5$ requires C, 35.82; H, 3.17; N, 5.22%). IR/Cm^{-1} (KBr): 1521 (C=N), 1420 (B−O), 2400 (B−H), 390 (Cu−O), 311 (Cu−Cl), 462 (Sn−Cl), 420 (Sn−N) 546 (Sn−C). (Scheme 1.)

Synthesis of **[$C_{32}H_{34}N_4S_2O_3BZnSn_2Cl_5$]** (6)

This was synthesized by a procedure similar to that described for complex [$C_{32}H_{34}N_4S_2O_3BCuSn_2Cl_5$] (5). Yield 0.50 g (59%) mp (dec.) 300 ± 3°C (found: C, 35.77; H, 3.16; N, 5.20. $C_{33}H_{40}N_4S_2O_7BZnSn_2Cl_5$ requires C, 35.75; H, 3.16; N, 5.21%). IR/Cm^{-1} (Nujol mull): 1524 (C=N), 1421 (B−O), 2400 (B−H), 402 (Zn−O), 320 (Zn−Cl), 460 (Sn−Cl), 428 (Sn−N), 549 (Sn−C). δ_H (300 MHz, DMSO, TMS) 7.67-6.62 (ArH), 9.84-8.40 (HC=N), 0.55 (B−H), 1.21 (CH_3). δ_c 130-124 (ArC), 168 (HC=N), 118 (C−N), 155 (C−S) 39.8 (Sn−C).

RESULT AND DISCUSSION

The reaction of Schiff base (1) with KBH_4 in 2 : 1 ratio yielded dihydro OO′ bis(salicylidene) 2,2′ aminobenzothiazolyl borate (2), which was utilized as a ligand for complexation with $CuCl_2$ (3), $ZnCl_2$ (4), and subsequent complexation of (3) and (4) with dimethyltindichloride yielded the bimetallic borate complexes (5) and (6), respectively.

All the complexes are air stable and are soluble in DMF, DMSO and are covalent in nature. The analytical data of the complexes conform to the structures proposed in Scheme 1.

IR spectra

The IR spectrum of the ligand shows prominent stretching vibration at 2372–2400 cm^{-1} region due to ν(B−H). The BH stretch generally appears as a single peak in the regions 2400–2500 cm^{-1}, but the presence of both ^{10}B and ^{11}B in natural boron results in the splitting of bands [22, 23]. Other characteristic frequencies due to the presence of the ligand appear at 1595 cm^{-1}, 1449 cm^{-1}, and 752 cm^{-1} assigned to ν(C=N), ν(C−N), and ν(C−S) vibrations, respectively [24–26]. The formation of borate is authenticated by the appearance of ν(B−O) band at 1391 cm^{-1} [27, 28], which is further confirmed by absence of ν(O−H) stretching vibration at 3422 cm^{-1} which was present in the Schiff base [29]. The ν(B−O) band, however, shifts to higher frequencies (28 cm^{-1}) in the complexes indicating the participation of oxygen of borate in the formation of complexes.

In the far IR spectra of the monometallic complexes, sharp absorption bands appearing at 390–402 cm^{-1}, 311–320 cm^{-1} are assigned to ν(M−O) and ν(M−Cl) vibration, respectively [30, 31]. The bimetallic complexes show absorption bands at 420–428, 546–549, and 460–462 cm^{-1} assigned to ν(Sn−N), ν(Sn−C), and ν(Sn−Cl), respectively, confirming the coordination of tin(IV) center to azomethine nitrogen and chlorine atoms [32, 33].

Electronic absorption spectra

The electronic absorption spectra of the borate ligand and complexes reveal three strong bands in 40 000–25 000 cm^{-1} region which are attributed to intraligand and charge transfer transitions.

The complex (3) exhibits a broad and low energy band at 16 528 cm^{-1} which is attributed to d-d transition ($^2B_{1g} \rightarrow {}^2A_{1g}$), typical for Cu^{II} in square planar environment. The absorption spectrum of the (5) complex exhibits two MLCT bands at 34 013 $cm^{-1}$and 30 303 cm^{-1} and a broad band at 17 361 cm^{-1} attributed to d-d transition which is typical for copper(II) complex in square planar geometry [34]. Although there is a shift in the d-d absorption band of the (5) complex in comparison to the absorption band observed for the (3) complex which is attributed to the presence of Sn(IV) metal ion, the environment around the copper center does not alter much, it retains square planar geometry.

EPR studies

The solid state X-band EPR spectrum of the Cu(II) complex recorded at LNT (77 K) was found to be anisotropic with only two peaks with "g" values $g_\perp = 2.037$, $g_\parallel = 2.195$, and $g_{av} = 2.089$, respectively. The parameter g_{av} was obtained according to the equation $[(g_{av}) = 1/3\ (g_\parallel + 2g_\perp)]$ and is in good agreement with corresponding anisotropy in square planar environment. The existence of $g_\parallel > g_\perp$ suggested that the unpaired electron is localized in $d_x{}^2\text{-}_y{}^2$ orbital of the Cu^{II} ion with "$3d^9$" configuration, that is, $(eg)^4$, $(a_1g)^2$ $(b_2g)^2$ $(b_1g)^1$, which is the characteristic of the square planar geometry [35].

The g values are related to the axial symmetry parameter G by the Hathaway [36, 37] expression $G = (g_\parallel - 2)/(g_\perp - 2)$. According to Hathaway, if the value of G is greater than four, the exchange interaction is negligible, whereas when the value of G is less than four, a considerable exchange interaction is indicated in the complex. In the complex (5), the G value obtained was 5.27 which indicates that exchange interactions are absent.

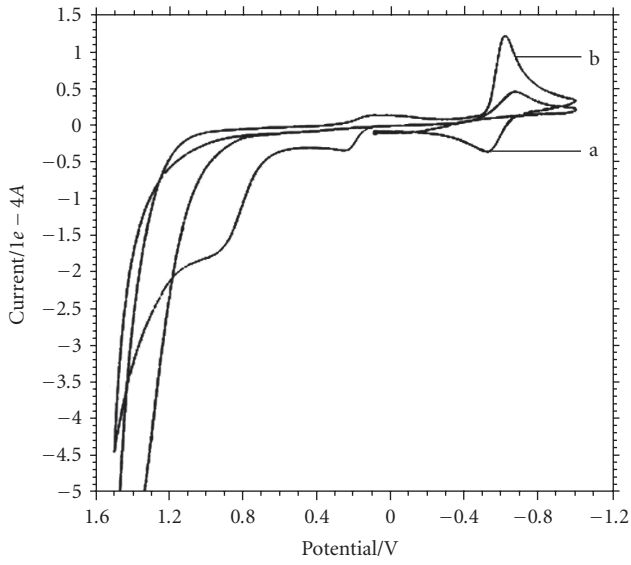

Figure 1: Cyclic voltammograms of the complex $C_{32}H_{34}N_4S_2O_3$-$BCuSn_2Cl_5$ (5) in (a) the absence and (b) the presence of guanine in DMSO/buffer (5 : 95) at a scan rate of 0.1 Vs^{-1}. Init E(V) = 0.1, high E(V) = 1.5, low E(V) = -1, Init P/N = P, scan rate (V/s) = 0.1, segment = 3, Smpl interval (V) = 0.001, quiet time (s) = 10, sensitivity (A/V) = 5e − 5.

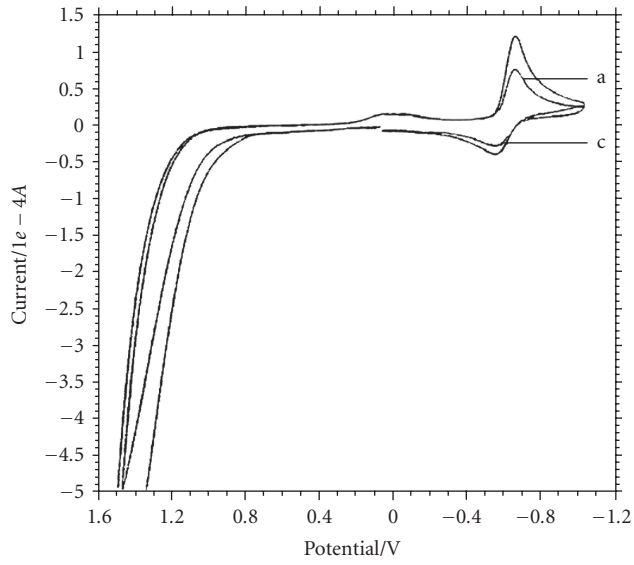

Figure 2: Cyclic voltammograms of the complex $C_{32}H_{34}N_4S_2O_3$-$BCuSn_2Cl_5$ (5) in (a) the absence and (b) the presence of adenine in DMSO/H_2O (5 : 95) at a scan rate of 0.1 Vs^{-1}. Init E(V) = 0.1, high E(V) = 1.5, low E(V) = -1, Init P/N = P, scan rate (V/s) = 0.1, segment = 3, Smpl interval (V) = 0.001, quiet time (s) = 10, sensitivity (A/V) = 5e − 5.

NMR studies

^{1}H NMR spectra are particularly useful to confirm the formation of borate ligand. The absence of phenolic −OH resonance peak at 10.12 ppm in the ligand clearly indicates the formation of borate by the removal of hydrogen gas [38] and the presence of BH_2 signal at 0.72 ppm [39]. The other signals due to N=CH proton and aromatic ring proton appear at 7.99-7.97 and 7.55-6.52 ppm, respectively. In the complexes (4) and (6), there is a slight upfield shift in BH_2 signal due to the presence of metal ions in the proximity of BH_2 protons. A new signal appears in the complex (6) at 1.21 ppm due to methyl protons of the dimethyltin moiety.

^{13}C NMR spectra of ligand have been recorded in DMSO and carbon resonance signals appears at 129-124, 165, 153, and 114 ppm assigned to aromatic phenyl ring carbons, HC=N, C−S, and C−N groups, respectively. Upon complexation, there is a slight shift in aromatic ring carbon resonance due to the coordination of metal to the oxygen atom of phenyl ring. Furthermore, complex (6) registers a new signal at 39.8 ppm attributed to $-Sn-CH_3$ carbons due to which CH=N carbon resonance gets altered slightly, this is also an indication of coordination of azomethine nitrogen to the diorganotindichloride. Other carbon signals remain unaltered in the complexes.

Electrochemical properties

The electrochemical behavior of the complex (5) has been examined by cyclic voltammetry to study the metallointeraction. The cyclic voltammogram of the complex (5) in absence of guanine, adenine, and calf thymus DNA was recorded in DMSO/H_2O (5 : 95) at a scan rate of 0.1 Vs^{-1} in the potential range −1.2 to 1.6 V versus Ag/AgCl electrode. It exhibits a well-defined quasireversible redox wave Cu^{II}/Cu^{I} attributed to one electron transfer process with E_p value at −0.615 V and −0.519 V (Figure 1, curve a). For this couple, the difference between the cathodic and anodic peak potentials ΔE_p is of the order 96 mV, a somewhat large peak to peak separations in comparison to Nernstian value (59 mV) observed for one electron transfer couple. Large peak width for one electron couple $Cu^{II} \rightarrow Cu^{I}$ is fairly common observation and is due to the reorganization of the coordination sphere during the electron transfer process [40, 41]. The ratio of anodic to cathodic peak currents I_{pa}/I_{pc} is less then the unity (0.3). The criteria for reversibility of the process is satisfied as on increasing the scan rate; the voltammogram does not show any significant change, and current is proportional to $V^{1/2}$ [42].

Table 1: Electrochemical data for complex (5) at a scan rate of 0.1 Vs^{-1} in the potential range −1.2 to 1.6 V.

System	E_{pc}	E_{pa}	$E_{1/2}$	I_{pa}/I_{pc}	ΔE_p
Complex (5) alone	−0.615 V	−0.519 V	−0.56 V	0.30	96 mV
Complex (5) + calf thymus DNA	−0.642 V	−0.561 V	−0.60 V	0.50	81 mV
Complex (5) + guanine	−0.669 V	—	—	—	—
Complex (5) + adenine	−0.617 V	−0.516 V	−0.56 V	0.50	101 mV

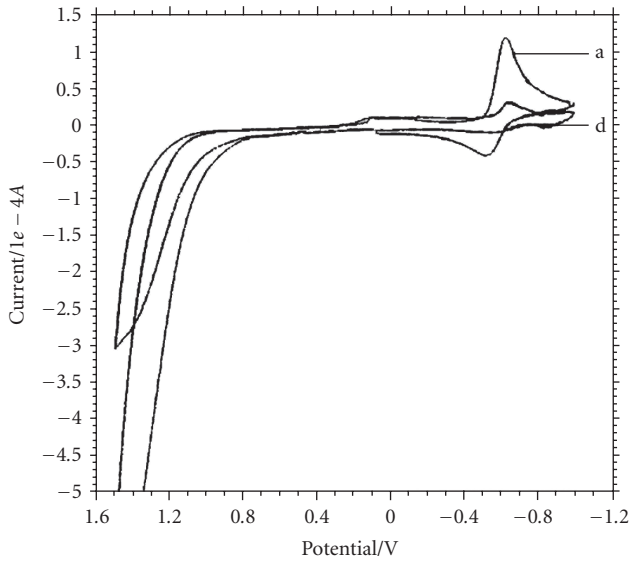

Figure 3: Cyclic voltammograms of the complex $C_{32}H_{34}N_4S_2O_3$-$BCuSn_2Cl_5$ (5) in (a) the absence and (b) the presence of calf thymus DNA in DMSO/buffer (5 : 95) at a scan rate of 0.1 Vs^{-1}. Init E(V) = 0.1, high E(V) = 1.5, low E(V) = -1, Init P/N = P, scan rate (V/s) = 0.1, segment = 3, Smpl interval (V) = 0.001, quiet time (s) = 10, sensitivity (A/V) = $5e-5$.

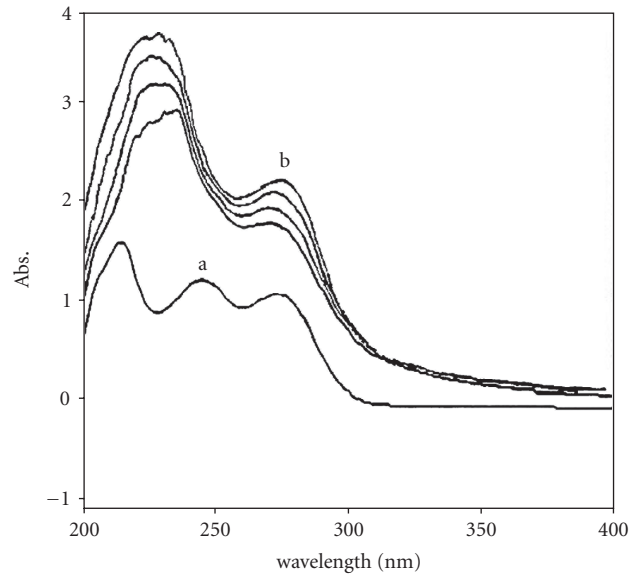

Figure 4: Absorption spectra of (a) guanine (1×10^{-3} M) dissolved in 9.2 pH buffer in the absence of the complex, (b) interaction of complex $C_{32}H_{34}N_4S_2O_3BCuSn_2Cl_5$ (5) with increasing amount of guanine.

The electrochemical behavior of the complex (5) in the presence of the guanine, adenine, and calf thymus DNA in DMSO/buffer, DMSO/H_2O, and DMSO/Tris buffer (5 : 95), respectively, are presented in Table 1.

The CV trace of the complex (5) in the presence of guanine shows a dramatic change in electrode potential E_p values, while the cathodic peak potential shifts to −0.669 V (in comparison to solution without guanine $E_p = -0.615$ V), a positive shift of −0.054 V is observed. However, the anodic peak disappear completely (Figure 1, curve b) indicative of strong binding of the complex to guanine base.

The cyclic voltammogram of the complex (5) in the presence of adenine shows a slight shift in formal potential values (in comparison to the solution in absence of adenine) (Figure 2, curve c). Although it corresponds fairly well with quasireversible one electron redox couple, peak potential does not show any significant change (0.002 and 0.003 V). The CV trace of adenine bound complex clearly suggests that the binding of the complex (5) to adenine is possible but the degree of binding is much lower in comparison to guanine.

However, the cyclic voltammogram of the complex (5) in the presence of calf thymus DNA (Figure 3, curve d) shows a significant shift in electrode potential value; cathodic and anodic peak potentials both shift to positive values −0.642 V and −0.561 V, while for the solution of the complex (5) in the absence of calf thymus DNA, electrode potential values are −0.615, −0.561 V as depicted in Figure 1, curve a, indicating that both the copper(II) and copper(I) forms interact with the calf thymus DNA to the same extent and suggest strong binding with calf thymus DNA [43]. Employing a square redox scheme, the net shift in $E_{1/2}$ has been estimated from the ratio of equilibrium constants for the binding of Cu^{II} and Cu^{I} complexes to calf thymus DNA using the following equation:

$$\begin{array}{ccc} Cu^{II} + e^- & \rightleftharpoons & Cu^{I} \\ {\scriptstyle K_{2+}}\Big\| & & \Big\|{\scriptstyle K_{1+}} \\ Cu^{II} - CTDNA + e^- & \rightleftharpoons & Cu^{I} - CTDNA \end{array} \qquad (1)$$

$$E^{I/2} - E^{1/2'} = 0.0591 \log(K_{1+}/K_{2+}),$$

where $E^{1/2}$ and $E^{1/2'}$ are formal potentials of the Cu(II)/Cu(I) couple in the free and bound forms, respectively. The ratios of binding constants of K_{2+} and K_{1+} were corresponding to binding constants for the Cu(II)/Cu(I) species to DNA, respectively [44]. The ratio of binding constants of 1+ and 2+ species was less than 1 (0.670 for calf thymus DNA), which provides an evidence for the preferential stabilization of Cu(II) species.

Kinetic studies

The interaction of the complex (5) with guanine, adenine, and calf thymus DNA in DMSO/buffer, DMSO/H_2O, and DMSO/Tris buffer (5 : 95) was studied spectrophotometrically at 25°C under pseudo-first-order conditions.

The electronic absorption spectrum of free guanine exhibits two characteristic bands at 244 nm and 273 nm. On addition of the complex (5), the UV band at 273 nm increased in intensity and shifted to 269 nm (a shift of 4 nm is observed), as shown in Figure 4. The binding of guanine with the complex (5) results in blue shift and increase in intensity

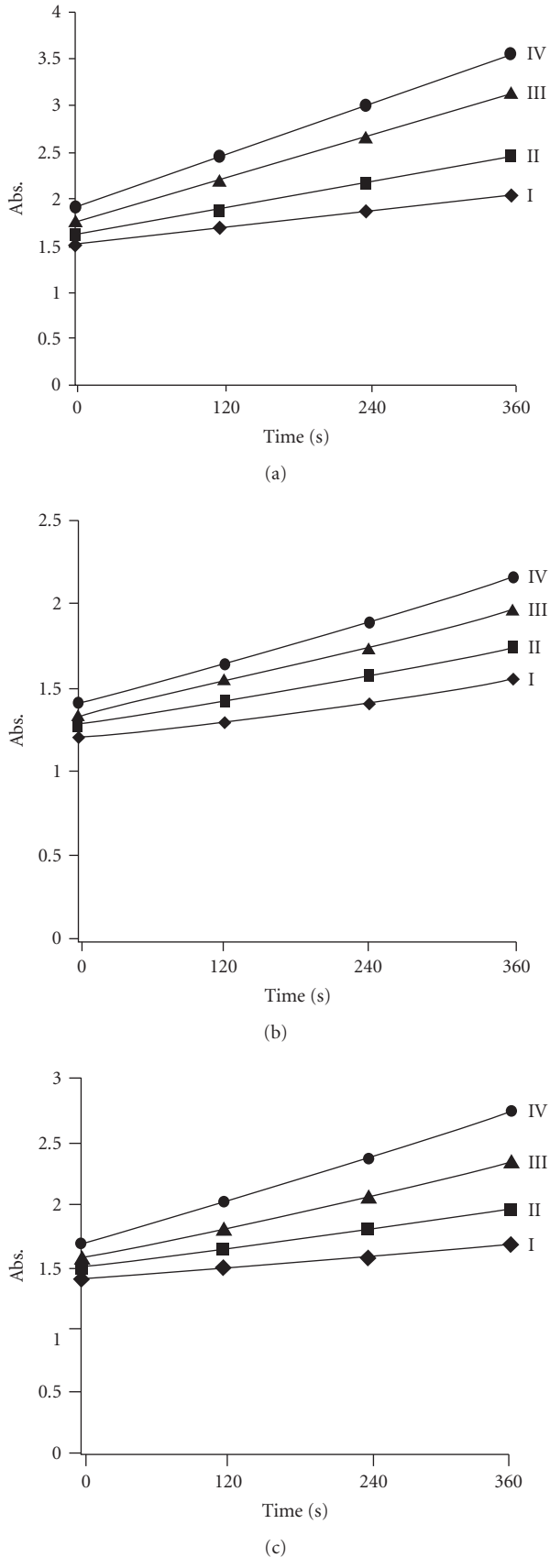

Figure 5: Plot of absorbance versus time at different concentrations of (a) guanine, (b) adenine, (c) calf thymus DNA.

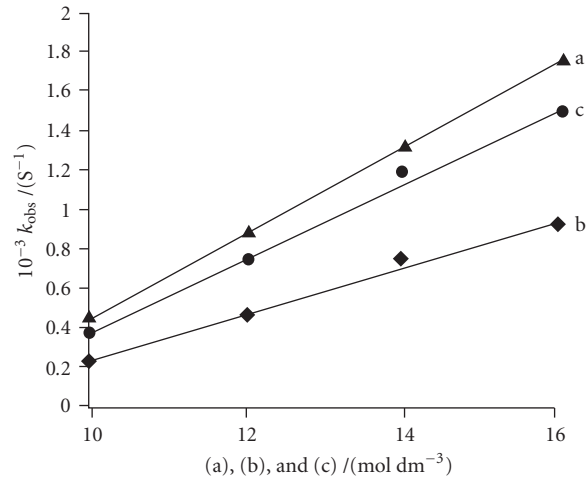

Figure 6: (a) Plot of k_{obs} versus guanine, (b) k_{obs} versus adenine, and (c) k_{obs} versus calf thymus DNA.

which is attributed to "hyperchromism." Hyperchromism was due to the breakage of intermolecular hydrogen bonds when bound to DNA and is consistent with many earlier reports for copper complexes [45, 46].

Kinetics of guanine binding to the complex (5) was studied at 269 nm (λ_{max} of the complex (5) + guanine) under pseudo-first-order condition keeping the concentration of complex constant ($c = 1 \times 10^{-3}$ M) and varying the concentration of guanine ($c = 10 - 16 \times 10^{-3}$ M) at different time intervals (Figure 5(a)). The rate constants k_{obs} were determined by the linear least squares regression method. An exponential $\log(A\alpha - A_0)$ of absorbance against time plots gave a straight line indicative of pseudo-first-order reaction upto 80% completion of the reaction (Figure 6).

The electronic absorption spectrum of adenine shows a characteristic UV band at 260 nm. On addition of the complex (5), there is no significant shift in wavelength and a slight increase in absorbance. Although a slight hyperchromism is observed, but the degree of hyperchromism is insignificant in comparison to the binding of guanine to the complex (5), which shows relatively weak interaction with adenine base.

Kinetics of adenine binding to the complex (5) was carried out at 260 nm (λ_{max} of complex (5) + adenine) under pseudo-first-order conditions. Figure 5(b) shows time scan plot of interaction of adenine with complex (5) depicting a small change in absorbance intensity. The rate constant k_{obs} values were plotted by linear least squares regression method (Figure 6).

The interaction of the complex (5) with calf thymus DNA was carried out to obtain detailed information concerning the magnitude of the kinetic influence from the DNA environment as a function of position of guanine N_7 within calf thymus DNA.

The interaction of the complex (5) to the calf thymus DNA was carried out at 260 nm (λ_{max} of calf thymus DNA) under pseudo-first-order conditions (Figure 5(c)). On addition of the complex (5) to the calf thymus DNA, absorption

spectra reveal a sharp change in absorption intensity with a red shift of 3 nm. At different time intervals, the absorption maxima increases in intensity indicating "hyperchromic effect" with calf thymus DNA.

The kinetics is further studied by observed pseudo-first-order rate constants k_{obs} value, as they can be directly compared and used as a measure of the kinetic influence from surrounding DNA [47]. The observed rate constant $1.77\,s^{-1}$ for guanine bound complex is of large magnitude in comparison to k_{obs} $1.52\,s^{-1}$ value for calf thymus DNA bound complex. The rate constant for adenine bound complex is $0.94\,s^{-1}$, which is much slow in comparison to guanine and calf thymus DNA. The complex shows preference for guanine over adenine due to two effects. When adenine binds, only a weak hydrogen bond is formed between the chloride ligand of the complex and H_2N-C_6 group of adenine; secondly, a significantly stronger molecular orbital interaction is identified in guanine in comparison to adenine. The presence of the electron withdrawing oxo group at the C_6 position of the purine ring lowers the energy of the lone-pair orbital at N_7 of purine base. The guanine molecular orbital has an energy of −6.877 eV, whereas −6.675 eV is obtained for adenine [48]. These studies have been demonstrated in a recent article of interaction of cisplatin with purine bases by Lippard et al [49]. Our investigations show that the complex $C_{32}H_{34}N_4S_2O_3BCuSn_2Cl_5$ is strongly bound to calf thymus DNA via different modes. Cu(II) prefers to bind strongly to N_7 of guanine base while the Sn^{IV} atom binds to the phosphate group [50]. Moreover, the affinity of Sn^{IV} with dinegative phosphate group is very strong due to its hard Lewis acidic nature. The binding to guanine is also kinetically preferred and supported by large k_{obs} value ($1.77\,s^{-1}$) for guanine bound complex.

Thus in conclusion, the complex (5) may first bind with phosphate group of calf thymus DNA, neutralize the negative charge of calf thymus DNA phosphate group, and cause contraction and conformation change of calf thymus DNA which is clearly evidenced by the "overall" hyperchromic effect observed in the absorption spectra.

ACKNOWLEDGMENTS

The author gratefully acknowledges CSIR, New Delhi, for financial support through research scheme no. 01(1722)/02/EMR-II. Special thanks are due to Dr. Sartaj Tabassum, Department of Chemistry, AMU, Aligarh, for providing valuable suggestions and cyclic voltammetry facilities. Thanks are also due to RSIC, Lucknow, for providing C, H, N, analysis data, IR, NMR, Mass spectra. We are grateful to RSIC, IIT Bombay, Mumbai, for EPR facilities.

REFERENCES

[1] Roberts JD, Peroutka J, Farrell N. Cellular pharmacology of polynuclear platinum anti-cancer agents. *Journal of Inorganic Biochemistry.* 1999;77(1-2):51–57.

[2] Farrell N, Qu Y, Bierbach U, Valsecchi M, Menta E. Structure-activity relationship within di- and trinuclear platinum phase I clinical agents. In: Lippert B, ed. *Cisplatin: Chemistry and Biochemistry of a Leading Anticancer Drug.* Weinheim, Germany: Wiley-VCH; 1999:479–496.

[3] Coluccia M, Nassi A, Boccarelli A, et al. In vitro anti-tumour activity and cellular pharmacological properties of the platinum-iminoether complex trans-$[PtCl_2[E - HN = C(OMe)Me]_2]$. *International Journal of Oncology.* 1999;15(5):1039–1044.

[4] Peti W, Pieper T, Sommer M, Keppler BK, Giester G. Synthesis of tumor-inhibiting complex salts containing the anion *trans*-tetrachlorobis(indazole)ruthenate(III) and crystal structure of the tetraphenylphosphonium salt. *European Journal of Inorganic Chemistry.* 1999;1999(9):1551–1555.

[5] Sullivan ST, Ciccarese A, Fanizzi FP, Marzilli LG. Cisplatin—DNA cross-link models with an unusual type of chirality-neutral chelate amine carrier ligand, *N,N′* dimethylpiperazine (Me_2ppz): Me_2ppzPt(guanosine monophosphate)$_2$ adducts that exhibit novel properties. *Inorganic Chemistry.* 2000;39(4):836–842.

[6] Vijayalakshmi R, Kanthimathi M, Subramanian V, Nair BU. Interaction of DNA with $[Cr(Schiff\ base)(H_2O)_2]ClO_4$. *Biochimica et Biophysica Acta (BBA)—General Subjects.* 2000;1475(2):157–162.

[7] Juskowiak B, Ohba M, Sato M, Takenaka S, Takagi M, Kondo H. Photoisomerizable DNA ligands. Spectral and electrochemical properties and base-pair selectivity of binding of bis[2-(1-alkylpyridinium-4-yl)vinyl]benzene dyes. *Bulletin of the Chemical Society of Japan.* 1999;72(2):265–277.

[8] Rodger A, Patel KK, Sanders KJ, Datt M, Sacht C, Hannon MJ. Anti-tumour platinum acylthiourea complexes and their interactions with DNA. *Journal of the Chemical Society, Dalton Transactions.* 2002;(19):3656–3663.

[9] Athar F, Arjmand F, Tabassum S. New asymmetric N2S2 macrocycles, their metal chelates and the photokinetics of DNA-complex interaction. *Transition Metal Chemistry.* 2001;26(4-5):426–429.

[10] Chauhan M, Arjmand F. Synthesis, characterization and interaction of a new chiral trinuclear complex trinuclear complex $[bis(aquodiaminotryptophanato)Cu^{II} - Sn_2^{IV}]$ chloride with calf thymus DNA. *Transition Metal Chemistry.* 2005;30:481–487.

[11] Baik M-H, Friesner RA, Lippard SJ. Theoretical study of cisplatin binding to purine bases: why does cisplatin prefer guanine over adenine? *Journal of the American Chemical Society.* 2003;125(46):14082–14092.

[12] Anderson FE, Duca CJ, Scudi JV. Some heterocyclic thiosemicarbazones. *Journal of the American Chemical Society.* 1951;73(10):4967–4968.

[13] Spielvogel BF, Sood A, Shaw BR, Hall IH. From boron analogues of amino acids to boronated DNA: potential new pharmaceuticals and neutron capture agents. *Pure and Applied Chemistry.* 1991;63(3):415–418.

[14] Biyala MK, Fahmi N, Singh RV. Reactivity and structural study of boron complexes with biochemical aspects. *Indian Journal of Chemistry.* 2004;43A(8):1662–1666.

[15] Soloway AH, Anisuzzaman AKM, Alam F, Barth RF, Liu L. The development of carboranyl nucleic acid precursors for use in neutron capture therapy of tumors. *Pure and Applied Chemistry.* 1991;63(3):411–413.

[16] Barbieri R, Alonzo GJ. The configuration and lattice dynamics of complexes of dialkyltin (IV) with adinosine 5′-monophosphate and phenyl phosphate. *Journal of the Chemical Society, Dalton Transactions.* 1987:789–794.

[17] Jancsó A, Nagy L, Moldrheim E, Sletten E. Potentiometric and spectroscopic evidence for co-ordination of dimethyltin(IV)

to phosphate groups of DNA fragments and related ligands. *Journal of the Chemical Society, Dalton Transactions.* 1999;(10): 1587–1594.

[18] Barbieri R, Silvestri A, Giuliani AM, Piro V, Simone FD, Madonia G. Organotin compounds and deoxyribonucleic acid. *Journal of the Chemical Society, Dalton Transactions.* 1992;(4):585–590.

[19] Höti N, Ma J, Tabassum S, Wang Y, Wu M. Triphenyl tin benzimidazolethiol, a novel antitumor agent, induces mitochondrial-mediated apoptosis in human cervical cancer cells via suppression of HPV-18 encoded E6. *The Journal of Biochemistry.* 2003;134(4):521–528.

[20] Huber F, Barbceri R. *Tin as a Vital Nutrient.* Boca Raton, Fla: CRC Press; 1986.

[21] Ghys L, Biesemans M, Gielen M, et al. Multinuclear 1D and 2D NMR investigations on the interaction between the pyrimidic nucleotides 5′-CMP, 5′-dCMP, and 5′-UMP and diethyltin dichloride in aqueous medium. *European Journal of Inorganic Chemistry.* 2000;2000(3):513–522.

[22] Pellei M, Pettinari C, Santini C, Skelton BW, Somers N, White AH. Synthesis, spectroscopic characterization, and structural systematics of new triorganophosphinecopper(I) poly(pyrazol-1-yl)borate complexes. *Journal of the Chemical Society, Dalton Transactions.* 2000;(19):3416–3424.

[23] Bould J, Kennedy JD, Ferguson G, Deeney FT, O'Riordan GM, Spalding TR. Metallaheteroborane chemistry: part 16. Contrasting metal to heteroborane bonding modes in isoelectronic $\{MC_2B_9\}$ and $\{MAs_2B_9\}$ clusters. Synthesis and characterisation of $[9-\{Fe(CO)_2(\eta 5-C_5H_5)\}-nido-7,8-C_2B_9H_{12}]$, $[7-\{Fe(CO)_2(\eta 5-C_5H_5)\}-nido-7,8-As_2B_9H_{10}]$ and $[7-\{M(CO)_2(\eta 7-C_7H_7)\}-nido-7,8-As_2B_9H_{10}]$, where M is Mo or W. *Dalton Transactions.* 2003;(23):4557–4564.

[24] Pasini A, Demartin F, Piovesana O, Chiari B, Cinti A, Crispu O. Novel copper(II) complexes of "short" salen homologues. Structure and magnetic properties of the tetranuclear complex $[Cu_2(L^2)_2]_2$ [H_2L^2 = phenyl-*N*,*N*′-bis(salicylidene) methanediamine]. *Journal of the Chemical Society, Dalton Transactions.* 2000;(19):3467–3472.

[25] Sevagapandian S, Rajagopal G, Nehru K, Athappan P. Copper(II), nickel(II), cobalt(II) and oxovanadium(IV) complexes of substituted β-hydroxyiminoanilides. *Transition Metal Chemistry.* 2000;25(4):388–393.

[26] Kumer A, Singh G, Handa RN, Dubey SN, Squattrito PJ. Synthesis and characterization of complexes of cobalt(II), Nickel(II), Copper(II) and Zinc(II) with Schiff Bases Derived from Cinnamaldehyde and 4-Amino-3-ethyl-5-mercapto-s-triazole and 4-Amino-5-mercapto-3-N-propyl-s-triazole. *Indian Journal of Chemistry.* 1999;38A:613.

[27] Tripathi SM, Tandon JP. Acetoxyboron derivatives of N-substituted salicylaldimines. *Journal of Inorganic and Nuclear Chemistry.* 1978;40(6):983–985.

[28] Pandey T, Singh RV. Synthesis structure elucidation and biological screening of unsymmetrical borate complexes of fluoroimines. *Synthesis and Reactivity in Inorganic and Metal-Organic Chemistry.* 2000;30:855–866.

[29] Bellamy LJ. *The Infrared Spectra of Complex Molecules.* 3rd ed. London, UK: Chapman & Hall; 1975.

[30] Nakamoto K. *Infrared and Raman Spectra of Inorganic and Coordination Compounds.* New York, NY: John Wiley & Sons; 1978.

[31] Chandra S, Singh G, Tyagi VP, Raizada S. Synthesis, esr, magnetic, and electronic spectral studies on manganese(II) complexes of semicarbazone and thiosemicarbazone. *Synthesis and Reactivity in Inorganic and Metal-Organic Chemistry.* 2001;31 (10):1759–1769.

[32] Jiazhu W, Jingshuo H, Liyiao H, Dashuang S, Shengzhi H. Antitumor activity of organotin compounds. Reaction, synthesis and structure of Et_2SnCl_2(phen) with 5-fluorouracil. *Inorganica Chimica Acta.* 1988;152(1):67–69.

[33] Gao E-Q, Bu W-M, Yang G-M, et al. Crystal structure, redox and spectral properties of copper(II) complexes with macrocyclic ligands incorporating both oxamido and imine groups. *Journal of the Chemical Society, Dalton Transactions.* 2000;(9):1431–1436.

[34] Raman N, Kulandaisamy A, Jeyasubramanian K. Synthesis, spectral, redox and biological studies of some Schiff base copper(II),nickel(II), cobalt(II), manganese(II), zinc(II) and oxovanadium(II) complexes derived from 1-phenyl-2,3-dimethyl-4 (4-iminopentan-2-one) pyrazol-5-one and 2-aminophenol/ 2-aminothiophenol. *Indian Journal of Chemistry.* 2002;41A:942–949.

[35] Jain MC, Srivastava AK, Jain PC. Some tetragonally distorted copper(II) complexes of 4-benzylamidothiosemicarbazide and its thiosemicarbazone. *Inorganica Chimica Acta.* 1977;23: 199–203.

[36] Hathaway BJ, Billing DE. The electronic properties and stereochemistry of mono-nuclear complexes of the copper(II) ion. *Coordination Chemistry Reviews.* 1970;5(2):143–207.

[37] Hathaway BJ. *Essays in Chemistry.* New York, NY: Academic Press; 1971. edited by JN Bradley and RD Gillard.

[38] Hoyos OL, Bermejo MR, Fondo M, et al. Mn(III) complexes with asymmetrical N_2O_3 Schiff bases. The unusual crystal structure of [Mn(phenglydisal-3-Br,5-Cl) (dmso)] (H_3phenglydisal = 3-aza-*N*-{2-[1-aza-2-(2-hydroxyphenyl) vinyl]phenyl}-4-(2-hydroxyphenyl)but-3-enamide), a mononuclear single-stranded helical manganese(III) complex. *Journal of the Chemical Society, Dalton Transactions.* 2000;(18): 3122–3127.

[39] Caballero A, Gómez-de la Torre F, Jalón FA, et al. Synthesis and characterisation of a series of ruthenium scorpionate complexes with B—H$\cdots$M agostic interactions. Crystal structure of [RuH(κ^2-*N*,*BH* Tp^{Tn})(PMe_3)(cod)] (Tp^{Tn} = hydrotris[3-(2-thienyl)pyrazol-1-yl]borate). *Journal of the Chemical Society, Dalton Transactions.* 2001;(4):427–433.

[40] Palaniandavar M, Pandiyan T, Lakshminarayanan M, Manohar H. Facial co-ordination in bis[bis(benzimidazol-2-ylmethyl)-amine]copper(II) perchlorate dihydrate. Synthesis, structure, spectra and redox behaviour. *Journal of the Chemical Society, Dalton Transactions.* 1995;(3):455–461.

[41] Mathur R, Mathur P. Monomeric Cu (II) complexes with tetradentate bis (benzimidazole) ligand ; synthesis, EPR, spectral and electrochemical studies. *Polyhedron.* 1998;17(16): 2607–2615.

[42] Hathaway BJ, Tomlinson AAG. Copper(II) ammonia complexes. *Coordination Chemistry Reviews.* 1970;5(1):1–43.

[43] Mahadevan S, Palaniandavar M. Chiral discrimination in the binding of tris(phenanthroline)ruthenium(II) to calf thymus DNA: an electrochemical study. *Bioconjugate Chemistry.* 1996;7(1):138–143.

[44] Lu X, Zhu K, Zhang M, Liu H, Kang J. Voltammetric studies of the interaction of transition-metal complexes with DNA. *Journal of Biochemical and Biophysical Methods.* 2002;52(3):189–200.

[45] Liu J, Zhang T, Lu T, et al. DNA-binding and cleavage studies of macrocyclic copper(II) complexes. *Journal of Inorganic Biochemistry.* 2002;91(1):269–276.

[46] Baldini M, Belicchi-Ferrari M, Bisceglie F, Pelosi G, Pinelli S, Tarasconi P. Cu(II) complexes with heterocyclic substituted thiosemicarbazones: the case of 5-formyluracil. Synthesis, characterization, x-ray structures, DNA interaction studies, and biological activity. *Inorganic Chemistry.* 2003;42(6):2049–2055.

[47] Sykfont Å, Ericson A, Elmroth SKC. Non-uniform rate for platination of guanine-N7 located in short DNA oligomers. *Chemical Communications.* 2001;(13):1190–1191.

[48] Baik M-H, Friesner RA, Lippard SJ. *cis*-$[Pt(NH_3)_2(L)]^{2+/+}$ (L = Cl, H_2O, NH_3) binding to purines and CO: does π-back-donation play a role? *Inorganic Chemistry.* 2003;42(26):8615–8617.

[49] Baik M-H, Friesner RA, Lippard SJ. Theoretical study of cisplatin binding to purine bases: why does cisplatin prefer guanine over adenine? *Journal of the American Chemical Society.* 2003;125(46):14082–14092.

[50] Thomas AM, Naik AD, Nethaji M, Chakravarty AR. Photoinduced DNA cleavage activity of ternary (N-salicylidene-L-methioninato)copper(II) complexes of phenanthroline bases. *Indian Journal of Chemistry.* 2004;43A(4):691–700.